JOURNAL OF AGRICULTURAL AND FOOD CHEMISTRY

Article

pubs.acs.org/JAFC

Structure and Physical Properties of Starch/Poly Vinyl Alcohol/ Laponite RD Nanocomposite Films

Xiaozhi Tang[†] and Sajid Alavi*[,‡]

[†]College of Food Science and Engineering, Nanjing University of Finance and Economics, Nanjing 210046, China

[‡]Department of Grain Science and Industry, Kansas State University, 201 Shellenberger Hall, Manhattan, Kansas 66506, United States

ABSTRACT: Nanocomposites of starch, poly vinyl alcohol (PVOH), and laponite RD (LRD) were produced by solution mixing and cast into films. In general, an increase in LRD content (0−20%) enhanced tensile strength and decreased water vapor permeability, irrespective of the relative humidity (50% and 75% RH). Tensile strength (TS) of starch/PVOH/LRD films ranged from 6.51 to 13.3 MPa. At 75% RH, TS was up to 65% higher as compared to films with sodium montmorillonite as filler. The most striking results were obtained with respect to elongation at break (*E*%), which ranged from 144% to 312%. Contrary to other polymer/clay nanocomposites, *E*% increased on addition of 5−20% LRD and was up to 175% higher than the control without clay. Nanocomposite structure and interactions were investigated using X-ray diffraction, transmission electron microscopy, and differential scanning calorimetry. Results indicated that LRD was a compatibilizer and cross-linking agent between polymers, and has the potential for use in biodegradable packaging films with good mechanical performance even in high humidity conditions.

KEYWORDS: *starch, poly vinyl alcohol, laponite, nanocomposite, biodegradable*

INTRODUCTION

Biodegradable packaging can provide a solution to the environmental impact of solid waste from petroleum-based packaging materials.[1] Demand for the former is increasing especially due to consumer awareness of the negative consequences of nondegradable and nonrenewable packaging.[2] Starch is a good candidate for replacing petroleum-based packaging materials as it has the unique advantage of being cheap, abundant, renewable, and biodegradable.[3] Starch can be used to form edible or biodegradable films with potential applications in food packaging. However, starch-based films are brittle in nature and also have poor water barrier properties.[4−6] These performance parameters exhibit further deterioration under conditions of high humidity. To overcome these drawbacks, researchers have employed various methods to improve barrier and mechanical properties of starch-based materials.

One successful technique involves blending of starch with other polymers, such as polycaprolactone,[7,8] polylactic acid,[9,10] and poly vinyl alcohol (PVOH).[1,11−13] Starch and PVOH blends are of particular interest because they are compatible and form hydrogen bonds easily.[14,15] Films from starch/PVOH blends are biodegradable and have improved mechanical properties over starch alone, although the latter is dependent on humidity. PVOH is also expensive and presents a poor barrier for moisture.

Another method for improving physical properties of starch-based films is the synthesis of nanocomposites using fillers such as layered silicates or clay.[5,6] Smectite clays like sodium montmorillonite (MMT) are the type mostly used in starch/clay nanocomposites due to their swelling properties and capacity to host water and organic molecules between platelet layers. Starch-based nanocomposites exhibit remarkable improvement in materials properties when compared to pristine starch or conventional micro- and macrocomposites.[5,6,16−19] These improvements can include increased modulus and strength, higher heat resistance, reduced moisture and gas permeability, and lower flammability.

A greater impact can be achieved by combining the two approaches described above to produce multicomponent nanocomposites such as those based on starch, PVOH, and MMT.[20−24] Dean et al.[20] utilized extrusion processing to synthesize thermoplastic starch/PVOH/MMT-based micro- and nanocomposites that exhibited intercalated and exfoliated structures. Use of small amounts of PVOH (up to 7 wt %) and MMT (up to 5 wt %) led to as much as 67% increase in tensile strength and 85% increase in tensile modulus. Vasile et al.[21] prepared starch/PVOH/MMT nanocomposites by the melt mixing method and reported a partially exfoliated morphology and slight increase in thermal stability of starch. In a recent study, solution mixing method was employed for the synthesis of starch/PVOH/MMT nanocomposite films with improved tensile strength and elongation properties as compared to films based on starch/MMT or starch alone.[22] Modifications to MMT, using alkyl ammonium cation and organic modifier citric acid, have been investigated as a means to improve mechanical properties of starch/PVOH/MMT nanocomposites produced by extrusion.[23] Surface modifications of starch/PVOH/MMT nanocomposites have been explored for improving biocompatibility in applications involving scaffolds for bone and cartilage tissue.[24] Despite enhancement in many properties, there exists room for further improvement in multicomponent nanocomposites. Their application in food packaging is of particular

Received: June 22, 2011
Revised: January 2, 2012
Accepted: January 3, 2012
Published: January 3, 2012

dx.doi.org/10.1021/jf2024962 | J. Agric. Food Chem. 2012, 60, 1954−1962

interest, but is still limited due to several reasons. For example, starch/PVOH-based nanocomposites have high water vapor permeability due to an abundance of hydroxyl groups in both base polymers; the presence of MMT tends to reduce elongational properties; and various physical properties deteriorate under high humidity conditions.

Clays other than MMT might lead to novel properties. Laponite is one such clay, which has not been investigated in the context of starch/PVOH-based nanocomposites. Laponite is a synthetic hydrous magnesium lithium silicate having the empirical formula $Na^{+}_{0.7}[(Mg_{5.5}Li_{0.3})Si_8O_{20}(OH)_4]^{-}_{0.7}$) and consisting of two tetrahedral silica sheets sandwiching a central octahedral magnesia sheet.[25−28] This smectite clay belongs to the hectorite family and has great capacity for swelling and exfoliation. Individual platelets of laponite have a diameter of ∼30 nm and thickness of ∼1 nm.[28]

This study focuses on starch/PVOH/laponite nanocomposites prepared by solution mixing. To investigate their application in flexible, biodegradable food packaging, these nanocomposites were cast into films, and various performance parameters were characterized including tensile strength, elongation at break, and water vapor permeability. Comparisons were made with starch/PVOH/MMT nanocomposites, to highlight the differences between laponite and MMT in terms of resultant matrix nanostructure, compatibility with starch/PVOH, and impact on physical properties.

MATERIALS AND METHODS

Materials. Normal corn starch (Cargill Inc., Cedar Rapids, IA) and polyvinyl alcohol (Elvanol 71-30; DuPont, Wilmington, DE) were the base polymers in all treatments. Elvanol 71-30 is a medium viscosity, fully hydrolyzed grade of polyvinyl alcohol. Other materials used in the synthesis of the nanocomposites included the nanoclays laponite and MMT (Southern Clay Products, Austin, TX) and the plasticizer glycerol (Sigma, St. Louis, MO). The laponite used was laponite RD or LRD, a particular gel-forming grade.[25,27]

Preparation of Nanocomposites and Film Casting. Aqueous starch/PVOH/clay solutions were prepared by mixing 6.7 g of starch, 3.3 g of PVOH, 3 g of glycerol, and LRD or MMT (0%, 5%, 10%, 15%, and 20% polymer basis) in 300 mL of water, and then heating this mixture at 95 °C for 30 min with constant stirring. The heated solution was cooled to 55 °C, and equal amounts were poured in Petri dishes. The water was allowed to evaporate by drying for 36−48 h at room temperature. The resulting films, having a thickness of around 0.1 mm, were peeled off and stored in airtight bags at room temperature for further tests.

X-ray Diffraction Analysis. The dispersion of clays in nanocomposite films was studied using X-ray diffraction (XRD). The X-ray diffractometer (D8 Advance; Bruker AXS GmbH, Karlsruhe, Germany) was operated at 40 kV and 40 mA. Scans were carried out at diffraction angles (2θ) of 1.0−10.0° with step size of 0.01° and scan speed of 4 s/step. X-ray radiation with a wavelength (λ) of 0.154 nm was generated from a Cu Kα source. The interlayer spacing or d-spacing of clay platelets was estimated from XRD scans by using Bragg's law as follows:

$$D = \frac{\lambda}{2\sin\theta} \tag{1}$$

where D is d-spacing (nm), λ is wavelength of X-ray beam (nm), and θ is the angle of incidence.

Transmission Electron Microscopy. Transmission electron microscopy (TEM) was used to visually observe clay dispersion in the nanocomposites. The electron microscope (CM100; Philips, Mahwah, NJ) was operated at 100 kV. Solution prepared for film casting was transferred to a carbon-coated copper grid and dried to make a film, which was then analyzed using TEM.

Thermal Analysis. The melting transition of nanocomposites was characterized using differential scanning calorimetry or DSC (Q100; TA Instruments, New Castle, DE). Films were conditioned by drying in an oven at 65 °C to achieve constant weight, and then sealed in airtight bags and stored at room temperature for further testing. Samples were weighed, hermetically sealed in aluminum pans, and heated from 10 to 250 °C at a rate of 10 °C/min. An empty aluminum pan was used as reference.

Water Vapor Permeability. Water vapor permeability was determined gravimetrically according to the standard method ASTM E96-00.[29] Films were fixed on top of test cells containing a desiccant (silica gel). The test cells were placed in a relative humidity chamber at 25 °C, and relative humidity (RH) of 50% or 75%. After steady-state conditions were reached, the weight of test cells was measured every 12 h over 3 days. The weight of the cells was plotted as a function of time for each sample, and the slope of the best-fit straight line ($\Delta G/\Delta t$) was used to calculate the water vapor transmission rate as follows:

$$\mathrm{WVTR} = \frac{\Delta G/\Delta t}{A} \tag{2}$$

where WVTR is the water vapor transmission rate (g/h·m^2), $\Delta G/\Delta t$ is the rate of weight change (g/h), and A is the test area (m^2). WVTR was then used to calculate the water vapor permeability as follows:

$$\mathrm{WVP} = \frac{\mathrm{WVTR} \times d}{\Delta P} \tag{3}$$

where WVP is the water vapor permeability (g·mm/kPa·h·m^2), d is the film thickness (mm), and ΔP is the partial pressure difference across the films (kPa).

Tensile Properties. Tensile properties of films were measured with a texture analyzer (TA-XT2; Stable Micro Systems Ltd., UK) using the standard method ASTM D882-02.[30] Films were cut into 2 cm × 8 cm strips and were conditioned at 23 °C and 50% or 75% RH for 3 days before testing. Ends of the test specimen were mounted on grips, and extension was carried out at a crosshead speed of 1 mm/s. Tensile strength (TS) and elongation at break (E%) were calculated as follows:

$$\mathrm{TS} = \frac{L_p}{a} \times 10^{-6} \tag{4}$$

where TS is tensile strength (MPa), L_p is peak load (N), and a is the cross-sectional area of samples (m^2).

$$E\% = \frac{\Delta L}{L} \times 100 \tag{5}$$

where ΔL is the increase in length at breaking point (mm), and L is the original length (mm).

Young's modulus (E) or the ratio of the tensile stress to tensile strain in the elastic (initial, linear) region of the stress−strain curve was calculated as follows:

$$E = \frac{FL}{a\Delta L'} \times 10^{-6} \tag{6}$$

where E is Young's modulus or modulus of elasticity (MPa), F is maximum force exerted in the elastic region (N), a is the original cross-sectional area of the film (m^2), and $\Delta L'$ is the increase in length in the elastic region (mm).

Experimental Design and Statistical Analysis. Nanocomposite synthesis and film casting experiments followed a 2 × 4 factorial design (two types and four levels of clay), with a control involving no clay. Thus, the experimental design comprised a total of nine treatments. Water vapor permeability and tensile properties of all films were determined at two levels of RH. Thus, the experimental design for these tests involved a total of 18 treatments. WVP tests were replicated three times, while tests for tensile properties were replicated five times. All data were analyzed using OriginLab scientific graphing and statistical analysis software (OriginLab Corp., Northampton, MA). Statistical significance of differences in means was determined using the Bonferroni LSD multiple-comparison method at $p < 0.05$.

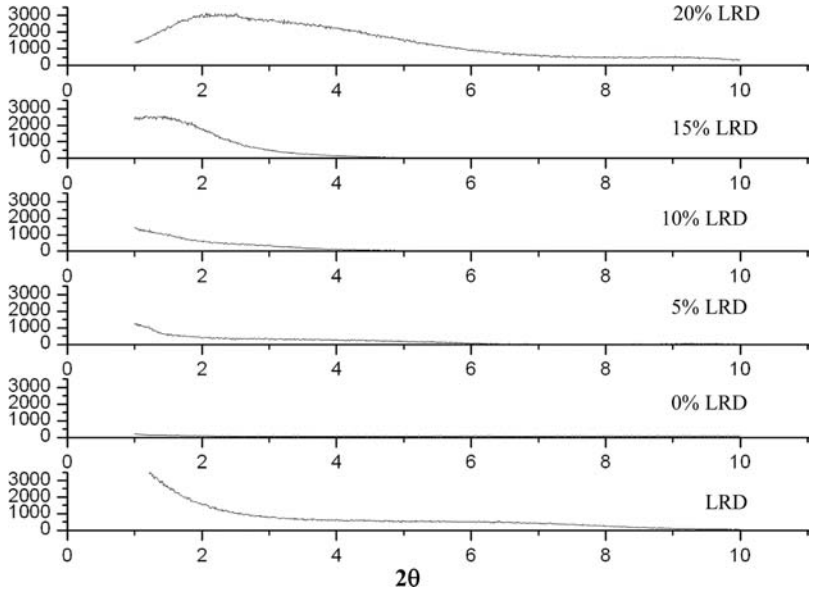

Figure 1. XRD patterns for pure laponite RD (bottom) and nanocomposites with 0−20% LRD.

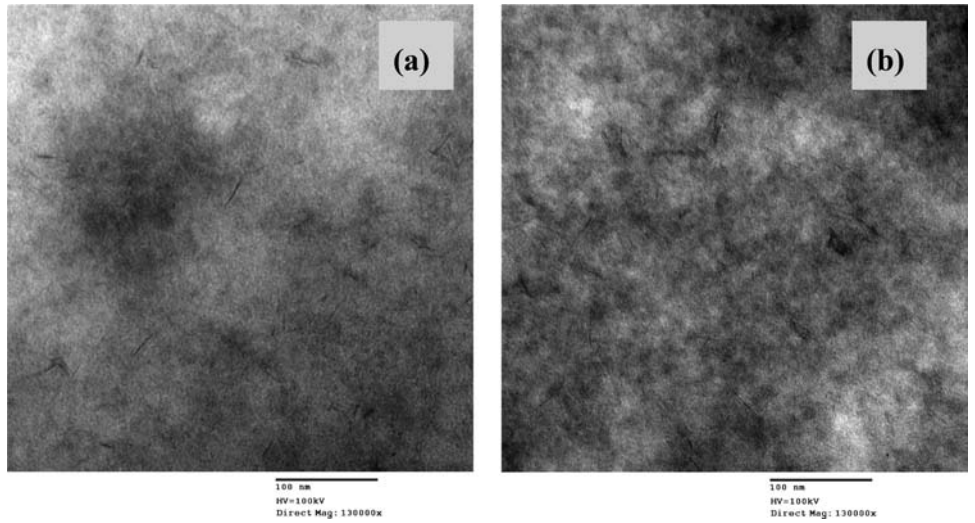

Figure 2. TEM images of nanocomposites with (a) 10% and (b) 20% LRD. The scale at the bottom represents 100 nm.

RESULTS AND DISCUSSION

Dispersion of LRD in Starch/PVOH Matrix. XRD patterns of polymer/clay composites or hybrids provide direct evidence of intercalated or exfoliated nanostructures.[5,6] Intercalated structures give rise to X-ray diffraction peaks because of the periodic and parallel assembly of silicate layers. The diffraction pattern of pristine LRD clay was almost flat, with a low intensity broadened peak at around $2\theta = 6.4°$ that corresponded to a *d*-spacing of 1.37 nm (Figure 1). Similar *d*-spacing (1.33−1.43 nm) was observed previously for laponite, although the corresponding diffraction peak was of much higher intensity due to ordered orientation of the basal plane in water-based films.[26,31] The broad diffraction pattern observed in the current study meant that the stacks of silicate platelets were not in a very ordered state, which is consistent with hectorite-type powders.[26] This is in contrast with natural MMT, which exhibits a well-ordered, layered nanostructure with a sharp XRD peak at 2θ of 7.1° (*d*-spacing of 1.24 nm).[22]

XRD patterns of starch/PVOH composite films with 0−20% LRD are also shown in Figure 1. The morphology of these hybrids, including the state of dispersion and *d*-spacing of silicate layers, varied with the level of incorporation of LRD. As expected, a featureless XRD pattern with no peak was observed for starch/PVOH alone (0% LRD) due to the absence of clay and the amorphous nature of melted PVOH and starch. Hybrids with 5% and 10% clay had very weak peaks around 2θ of 1.2° (*d*-spacing of 7.35 nm) and 1.4° (*d*-spacing of 6.30 nm), respectively. This indicated that polymer chains could enter the silicate layers and push them apart, resulting in a higher degree of disorder and exfoliation than pristine LRD. A diffraction peak of much higher intensity was observed for 15% LRD, corresponding to 2θ of 1.6° (*d*-spacing of 5.51 nm). This hybrid had a distinct dual structure, indicating the coexistence of exfoliation and aggregation of silicate layers in the polymer matrix. A very intense XRD peak at $2\theta = 2.3°$ (*d*-spacing of 3.84 nm) was observed at 20% LRD, suggesting that a highly ordered and aggregated layered structure was induced. Thus, in comparison with 5% and 10% LRD, higher clay content not only led to lower *d*-spacing or lesser separation of silicate layers, but also caused aggregation rather than the random distribution

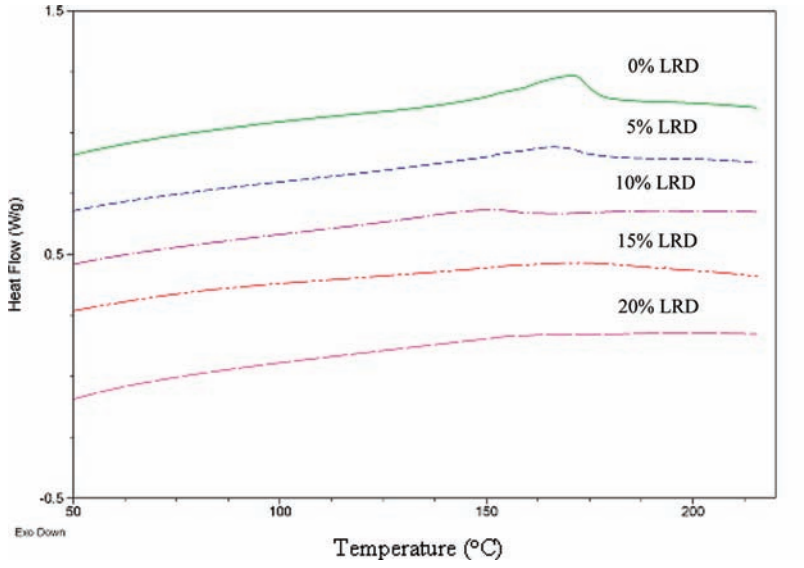

Figure 3. DSC scans showing melting peaks for nanocomposites with 0–20% LRD.

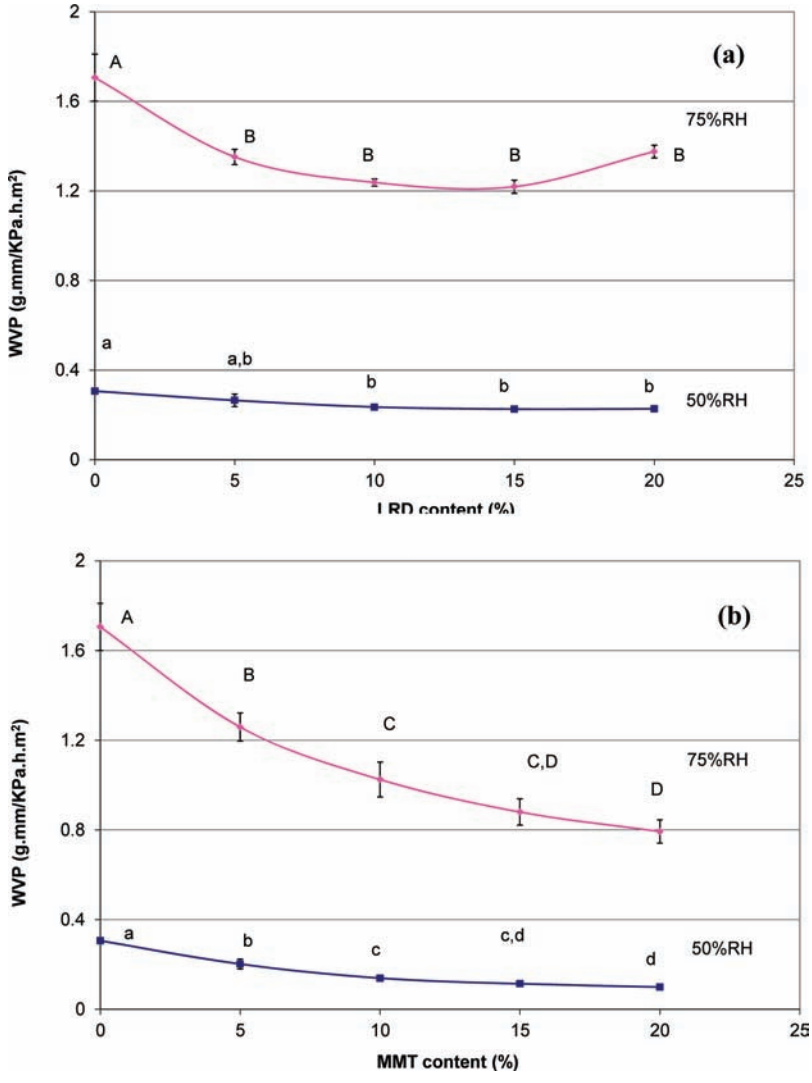

Figure 4. Water vapor permeability (WVP) of starch/PVOH-based nanocomposite films with (a) laponite RD and (b) sodium montmorillonite as filler. Error bars indicate standard deviation. Data points with different letters imply significant difference ($p < 0.05$).

dx.doi.org/10.1021/jf2024962 | J. Agric. Food Chem. 2012, 60, 1954–1962

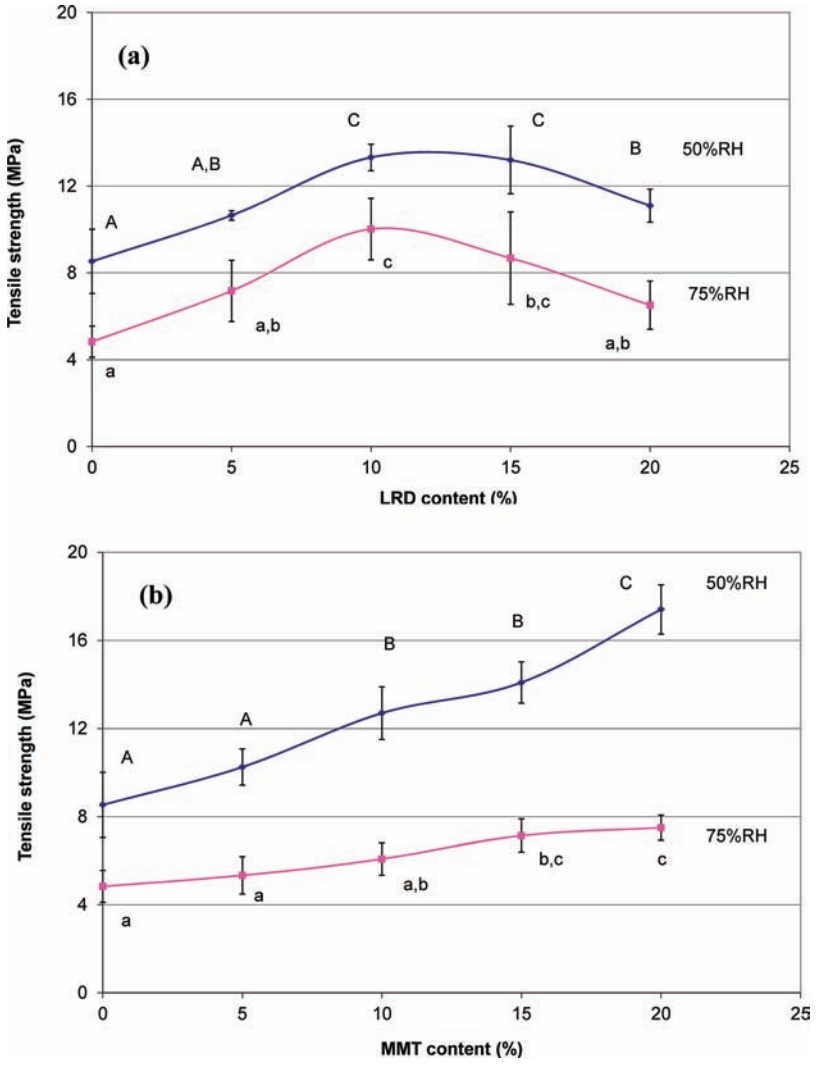

Figure 5. Tensile strength of starch/PVOH-based nanocomposite films with (a) laponite RD and (b) sodium montmorillonite as filler. Error bars indicate standard deviation. Data points with different letters imply significant difference ($p < 0.05$).

of clay platelets found in original LRD. This is a unique observation, and differs from hybrids based on other types of clay including starch/PVOH/MMT nanocomposites. Irrespective of the clay content, the latter have been shown to have greater dispersion of silicate layers as compared to natural MMT.[22]

Transmission electron microscopy images of starch/PVOH/LRD nanocomposites are shown in Figure 2. The morphologies revealed by TEM corresponded well to the inferences drawn from XRD analysis. At 10% clay content, individual laponite platelets were randomly dispersed in the polymer matrix. This confirmed a high degree of disorder and exfoliation, although there were some unexfoliated platelets or tactoids that remained. For the hybrid with 20% laponite, more integrated and tightly stacked layered structures were visible throughout the matrix. In general, the starch/PVOH polymer matrix and LRD are both hydrophilic and compatible with each other, leading to good dispersion of the latter at low concentrations. However, electrostatic interactions between edges and surfaces of adjacent laponite platelets might induce stacking and agglomeration at higher concentrations.[27] This could be the reason for poor clay dispersion at LRD contents higher than 10%.

Thermal Characterization. DSC thermograms of starch/PVOH/LRD hybrid films are shown in Figure 3. On addition of LRD, a decrease in melting temperature and broadening of the melting peaks were observed. Laponite may function as a compatibilizer and increase the miscibility of PVOH with starch. Hybrids with 5% and 10% LRD had good dispersion of clay as discussed earlier, and thus improved the homogeneity of the polymer matrix and promoted interactions in the multicomponent system. Increased interaction of PVOH with starch and laponite would disrupt the rigid arrangement of PVOH chains and decrease its crystallinity, which could explain the changes in melting characteristics. In fact, laponite can have a cross-linking action on polymers.[28] Broadening in melting peaks of starch/PVPH blends due to cross-linking and/or interactions between starch and PVOH has been reported earlier, although these studies did not involve laponite.[13,22]

For hybrids with 15% and 20% LRD, the melting peaks were indistinct as the melt transition was too weak and broad to measure. This absence of thermal events was due to the confinement of entire polymer in interlayer spaces of laponite, and the absence of bulk-like PVOH.[32]

Barrier Properties. Water vapor permeability data for starch/PVOH/LRD and starch/PVOH/MMT hybrid films are

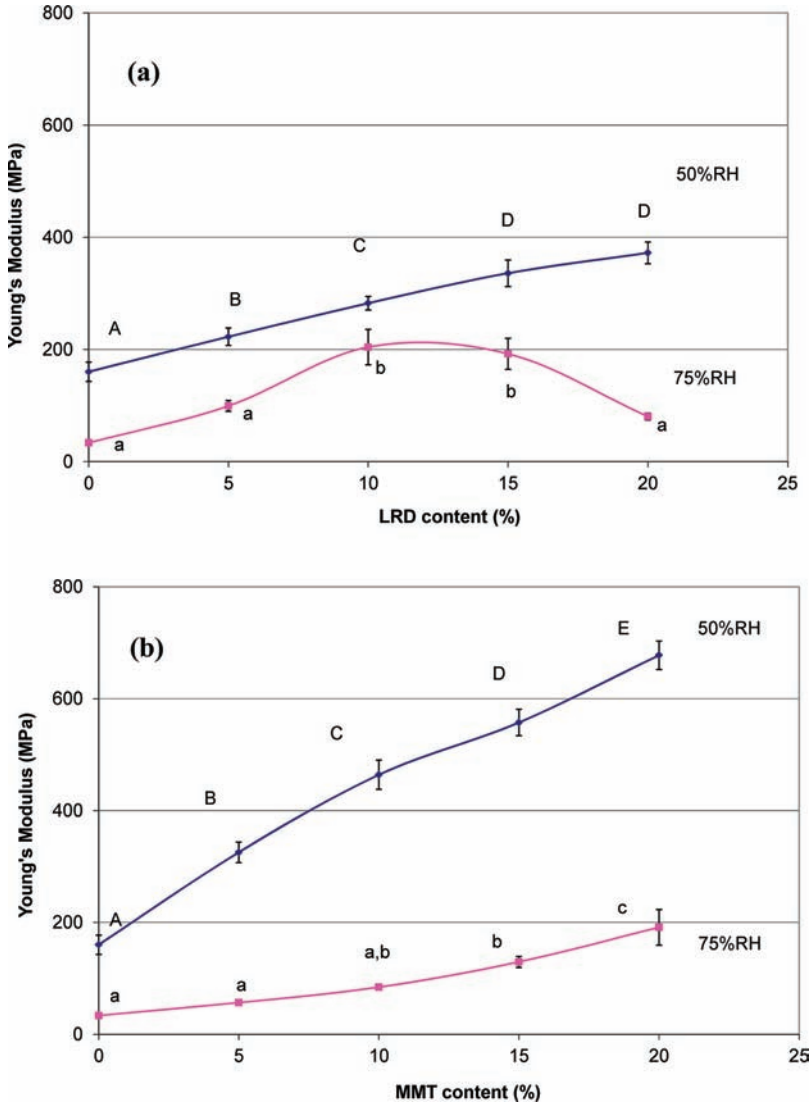

Figure 6. Young's modulus of starch/PVOH-based nanocomposite films with (a) laponite RD and (b) sodium montmorillonite as filler. Error bars indicate standard deviation. Data points with different letters imply significant difference ($p < 0.05$).

shown in Figure 4. In the case of the former, WVP at 50% RH decreased from 0.306 to 0.226 g·mm/kPa·h·m^2 as LRD content increased from 0% to 15%. This was due to increase in the effective path length for diffusion and is a typical observation in intercalated or exfoliated polymer/clay systems.[5,22,25,33,34] WVP remained almost unchanged at 0.227 g·mm/kPa·h·m^2 on further increase of LRD to 20%. The aggregated structure of LRD possibly provided channels or microvoids at the interface of polymer and clay, thus compensating for increase in tortuosity.[22] Higher WVP was observed at 75% RH as compared to 50% RH. As humidity increases, films are hydrated to a greater extent. The water, acting as a plasticizer, loosens the polymeric matrix and facilitates higher diffusion rates. The effect of clay content was also more pronounced at 75% RH, with decrease in WVP from 1.71 to 1.22 g·mm/kPa·h·m^2 as LRD content increased from 0% to 15%. However, WVP increased to 1.38 g·mm/kPa·h·m^2 on further increase of LRD to 20% due to domination of the clay aggregation effect.

In general, WVP for starch/PVOH/MMT hybrid films was lower as compared to starch/PVOH/LRD films, implying that the former possessed better barrier properties. The enhanced barrier characteristics result from higher aspect ratio of MMT (~100) as compared to LRD (~30). The overall trends for WVP of starch/PVOH/MMT films, with respect to clay content and relative humidity, were similar to starch/PVOH/LRD films. As MMT content increased from 0% to 20%, WVP decreased from 1.71 to 0.793 g·mm/kPa·h·m^2 and from 0.306 to 0.099 g·mm/kPa·h·m^2 at RH of 75% and 50%, respectively. However, unlike laponite, the decreasing trend for WVP was not halted or reversed at 20% clay content, possibly due to better dispersion of montmorillonite.

Mechanical Properties. Tensile strength (TS) data for starch/PVOH/LRD and starch/PVOH/MMT hybrid films are shown in Figure 5. TS of starch/PVOH/LRD films at 50% RH increased from 8.53 to 13.3 MPa with increase in laponite content from 0% to 10%. Such an improvement in mechanical strength is commonly observed in nanocomposite materials and is related to adequate dispersion and higher strength of clay nanoparticles that act as reinforcing fillers.[22,35,36] The coupling between the tremendous surface area of the clay and the polymer matrix facilitates development of constrained regions with high stiffness, transfer of stress to the reinforcement phase, and consequently enhancement of tensile strength of the nanocomposite. Increase in laponite content beyond 10%,

dx.doi.org/10.1021/jf2024962 | J. Agric. Food Chem. 2012, 60, 1954−1962

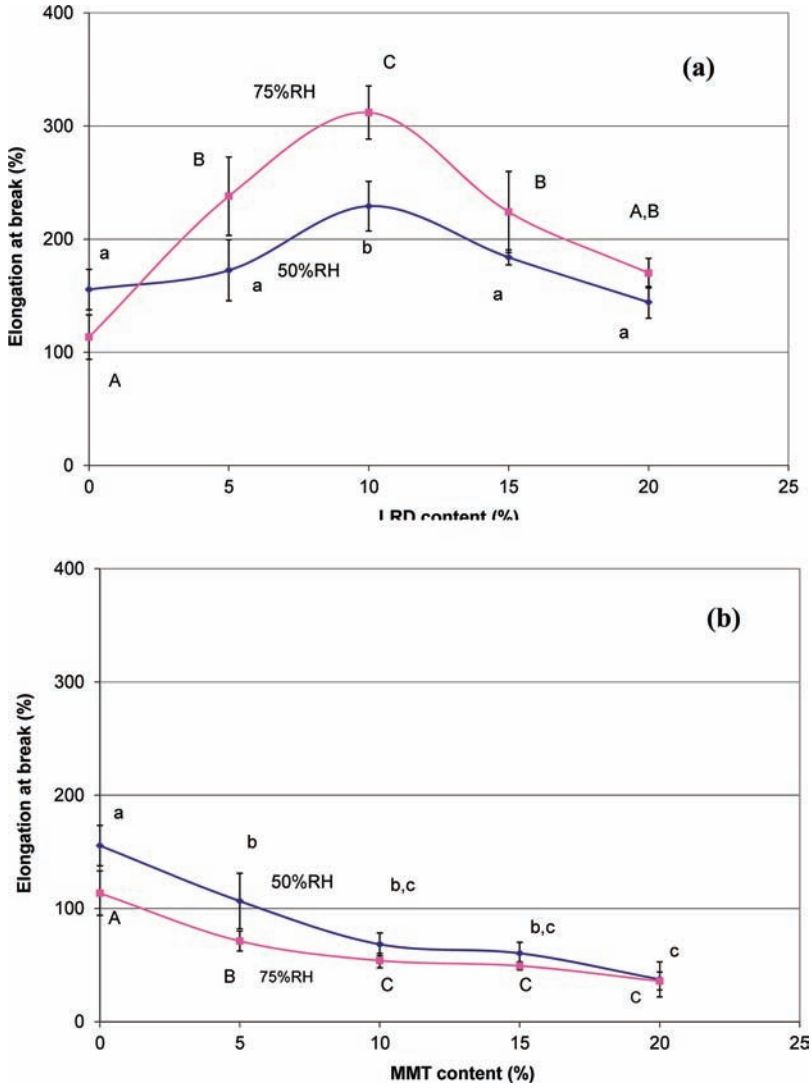

Figure 7. Elongation at break of starch/PVOH-based nanocomposite films with (a) laponite RD and (b) sodium montmorillonite as filler. Error bars indicate standard deviation. Data points with different letters imply significant difference ($p < 0.05$).

however, led to decrease in TS. The hybrid containing 20% LRD had tensile strength of 11.1 MPa, which was still higher than the control (0% LRD). As described earlier, at higher LRD contents (15% and 20%), the degree of exfoliation decreased, and more aggregated clay structures were formed. This aggregation disrupted the continuous phase of starch/PVOH polymer matrix and also decreased the exposed clay surface area, thus decreasing the tensile strength. Similar trends were observed at 75% RH, although films tested at the higher relative humidity had lower TS. At higher RH, the polymer matrix absorbs more water, which acts as a plasticizer and weakens the polymer matrix. A part of the water is also adsorbed on the clay surface, thus negatively affecting nanofiller−matrix affinity and the transfer of clay platelet rigidity to the matrix.[37]

A similar trend with respect to humidity was observed for tensile strength of starch/PVOH/MMT films. However, irrespective of RH and in contrast to films with laponite as nanofiller, TS of starch/PVOH/MMT films exhibited a monotonic increase as montmorillonite content increased from 0% to 20%. This again points to a better dispersion or exfoliation/intercalation of MMT platelets even at high loadings of 15−20%. The highest TS of 17.4 and 7.50 MPa, at 50% and 75% RH, respectively, was observed at 20% MMT. Interestingly, at lower clay loading (up to 10%), TS of starch/PVOH/LRD films was up to 65% higher than starch/PVOH/MMT. The difference was more pronounced at 75% RH, indicating greater effectiveness of laponite as a reinforcing filler, especially in conditions of high relative humidity. Differences between the two clays with respect to affinity to polymer matrix and rigidity of platelets could be contributing factors.

In general, Young's modulus data (Figure 6) for the nanocomposite films followed trends similar to those of tensile strength, with respect to nanofiller type and content, and also relative humidity. The underlying reasons are also similar, as Young's modulus can be considered a measure of the tensile strength in the initial elastic region of the force-deformation response. The modulus monotonically increased with increase in clay content, except in the case of starch/clay/LRD films tested at higher humidity (75% RH) conditions. As discussed earlier, the enhancement of Young's modulus can be attributed to the higher modulus of the clay platelets and their dispersion in the polymer matrix. The latter contributes to the affinity and adhesion of the polymers to the filler surface. Contrary to the general observation, Young's modulus decreased at 75% RH

dx.doi.org/10.1021/jf2024962 | J. Agric. Food Chem. 2012, 60, 1954−1962

when LRD content was higher than 10%. This could be a result of decrease in available surface area for polymer/clay interactions at high loading of laponite caused by aggregation of platelets and lower effective modulus of nanofiller at higher humidity due to the adsorption of water molecules to the clay surface. The effective stiffness modulus of clay takes into account the affinity between the nanofiller and the matrix, and has been shown to decrease with rise in relative humidity using a modeling-based approach.[37] Young's modulus at 50% RH ranged from 160 to 372 MPa and 160 to 678 MPa for LRD and MMT as nanofillers, respectively. It was much lower at 75% RH, ranging from 33.6 to 204 MPa and 33.6 to 191.5 MPa, respectively. The combination of reduced effective modulus of clay and plasticization of the hydrophilic polymer matrix contributed to the lower modulus at higher humidity. It was also interesting to observe that at 75% RH and up to 15% clay loading, the modulus of starch/PVOH/LRD films was higher than starch/PVOH/MMT. Reasons similar to those discussed for tensile strength are applicable. However, at lower humidity, incorporation of MMT led to a far greater enhancement in Young's modulus than LRD. This was contrary to the observation for tensile strength. Deformation beyond the elastic region was taken into account for characterization of tensile strength, and laponite has advantages over montmorillonite at larger-scale deformations due to its role as a compatibilizer and cross-linker, which is discussed next in more detail.

Elongation at break (*E*%) data for the nanocomposite films are shown in Figure 7. *E*% decreased from 156% to 37.4% as MMT content increased from 0% to 20%, at 50% RH. The corresponding decrease at 75% RH was from 114% to 35.9%. Similar reduction in extensibility or elongation properties with increase in nanofiller content has been observed for various polymer/clay nanocomposites.[5,22,36] The clay−polymer interactions prevent easy sliding of polymer chains against each other, thus lowering *E*%. A sharper decrease in *E*% was observed between 0% and 10% MMT because of better dispersion of the clay at lower content. Elongation at break for starch/PVOH/MMT films decreased at higher humidity level (75% RH) due to the weakening of the polymer matrix with more water absorption.

Starch/PVOH/LRD nanocomposite films had much higher extensibility than films with MMT as nanofiller. *E*% for the former ranged from 144% to 229% at 50% RH and from 170% to 312% at 75% RH. Also, contrary to trends observed for typical polymer/clay nanocomposites, elongation at break increased significantly as compared to the control on addition of 5−20% LRD. Films with 10% LRD had the highest *E*%, with almost 3-fold increase at 75% RH. These results point to a very different mechanism for interactions between laponite and the polymer matrix, as compared to other clays such as MMT. The cross-linking action of laponite on polymers and its role as a compatibilizer between starch and PVOH were discussed earlier in the context of weakening of melt transition of the nanocomposites. The increase in elongational properties of laponite-reinforced polymer matrices, such as hydrogels, fibers, and films, has also been attributed to physical cross-linking.[28,38,39] Polymer chains get adsorbed to the charged nanoplatelet surfaces via interactions like hydrogen bonding and ionic attraction, thus forming a cross-linked, viscoelastic network and leading to enhanced elongation during mechanical deformation. This process was aided by the smaller size of laponite platelets and their homogeneous dispersion at clay loading up to 10%. However, with further increase of LRD content, the homogeneous phase was disrupted by aggregation of silicate layers and resulted in the decrease of elongation at break. Also, contrary to MMT-reinforced films, *E*% for starch/PVOH/LRD was greater at the higher RH. Increased mobility due to the plasticizing effect of water could have led to enhanced interaction between polymer chains and platelet surfaces, and thus enhanced degree of cross-linking.

In conclusion, the impact of the nanofiller laponite RD on properties of starch/PVOH films was analyzed. Starch/PVOH/LRD nanocomposites had a high degree of exfoliation at lower clay content (up to 10%), which meant LRD was well dispersed in the polymer matrix. However, at higher LRD content, the silicate platelets were aggregated. The addition of LRD improved both water barrier and mechanical properties of the nanocomposite films. Contrary to most polymer/clay systems, a significant increase in elongation at break was detected with increase in filler content due to the unique function of laponite as a cross-linking agent and compatibilizer between starch and PVOH. Starch/PVOH/LRD-based nanocomposites have promising potential as a low cost, biodgradeable alternative to conventional plastics in flexible packaging applications for food products. Enhanced extensibility, higher tensile strength, and reduced deterioration in performance at high humidity conditions are some of the advantages over nanocomposites based on other clays such as MMT.

AUTHOR INFORMATION

Corresponding Author

*Tel.: (785) 532-2043. Fax: (785) 532-4017. E-mail: salavi@ksu.edu.

Funding

This project was supported by the National Research Initiative Competitive Grants Program of the United States Department of Agriculture, grant number 20081503. This is contribution number 11-137-J from the Kansas Agricultural Experiment Station, Manhattan, KS 66506.

REFERENCES

(1) Jayasekara, R.; Harding, I.; Bowater, I.; Christie, G. B. Y.; Lonergan, G. T. Preparation, surface modification and characterization of solution cast starch PVA blended films. *Polym. Test.* **2004**, *23*, 17−27.

(2) Elizondo, N. J.; Sobral, P. J. A.; Menegalli, F. C. Development of films based on blends of Amaranthus cruentus flour and poly(vinyl alcohol). *Carbohydr. Polym.* **2009**, *75*, 592−598.

(3) Averous, L. Biodegradable multiphase systems based on plasticized starch: A review. *J. Macromol. Sci., Polym. Rev.* **2004**, *C44*, 231−274.

(4) Dean, K.; Yu, L.; Wu, Y. D. Preparation and characterization of melt-extruded thermoplastic starch/clay nanocomposites. *Compos. Sci. Technol.* **2007**, *67*, 413−421.

(5) Tang, X. Z.; Alavi, S.; Herald, T. J. Barrier and mechanical properties of starch-clay nanocomposite films. *Cereal Chem.* **2008**, *85*, 433−439.

(6) Tang, X. Z.; Alavi, S.; Herald, T. J. Effect of plasticizers on the structure and properties of starch-clay nanocomposite films. *Carbohydr. Polym.* **2008**, *74*, 552−558.

(7) Koenig, M. F.; Huang, S. T. Biodegradable blends and composites of polycaprolactone and starch derivatives. *Polymer* **1995**, *36*, 1877−1882.

(8) Averous, L.; Moro, L.; Dole, P.; Fringant, C. Properties of thermoplastic blends: starch−polycaprolactone. *Polymer* **2000**, *41*, 4157−4167.

(9) Chang, J. L. Reactive blending of biodegradable polymers: PLA and starch. *J. Polym. Environ.* **2004**, *8*, 33−37.
(10) Jang, W. Y.; Shin, B. Y.; Lee, T. J.; Narayan, R. Thermal properties and morphology of biodegradable PLA/starch compatibilized blends. *J. Ind. Eng. Chem.* **2007**, *13*, 457−464.
(11) Mao, L.; Imam, S.; Gordon, S.; Cinelli, P.; Chiellini, E. Extruded cornstarch-glycerol-polyvinyl alcohol blends: Mechanical properties, morphology and biodegradability. *J. Polym. Environ.* **2002**, *8*, 205−211.
(12) Yang, S. Y.; Huang, C. Y. Plasma treatment for enhancing mechanical and thermal properties of biodegradable PVA/starch blends. *J. Appl. Polym. Sci.* **2008**, *109*, 2452−2459.
(13) Zou, G. X.; Qu, J. P.; Zou, X. L. Extruded starch/PVA composites: water resistance, thermal properties and morphology. *J. Elastomers Plast.* **2008**, *40*, 303−316.
(14) Sin, L. T.; Rahman, W. A. W. A.; Rahmat, A. R.; Khan, M. I. Detection of synergistic interactions of polyvinyl alcohol-cassava starch blends through DSC. *Carbohydr. Polym.* **2010**, *79*, 224−226.
(15) Zhou, Y. X.; Cui, F. Y.; Jia, D. M.; Xie, D. Effect of complex plasticizer on the structure and properties of the thermoplastic PVA/starch blends. *Polym.-Plast. Technol. Eng.* **2009**, *48*, 489−495.
(16) Park, H.; Li, X.; Jin, C.; Park, C.; Cho, W.; Ha, C. Preparation and properties of biodegradable thermoplastic starch/clay hybrids. *Macromol. Mater. Eng.* **2002**, *287*, 553−558.
(17) Park, H.; Lee, W.; Park, C.; Cho, W.; Ha, C. Enviromentally friendly polymer hybrids part 1. Mechanical, thermal and barrier properties of thermoplastic starch/clay nanocomposites. *J. Mater. Sci.* **2003**, *38*, 909−915.
(18) Avella, M.; De Vlieger, J. J.; Errico, M. E.; Fischer, S.; Vacca, P.; Volpe, M. G. Biodegradable starch/clay nanocomposite films for food packaging applications. *Food Chem.* **2005**, *93*, 467−474.
(19) Chivrac, F.; Pollet, E.; Schmutz, M.; Averous, L. New approach to elaborate exfoliated starch-based nanobiocomposites. *Biomacromolecules* **2008**, *9*, 896−900.
(20) Dean, K. M.; Do, M. D.; Petinakis, E.; Yu, L. Key interaction in biodegradable thermoplastic starch/poly (vinyl alcohol)/montmorillonite micro and nanocomposites. *Compos. Sci. Technol.* **2008**, *68*, 1453−1462.
(21) Vasile, C.; Stoleriu, A.; Popescu, M.; Duncianu, C.; Kelnar, I.; Dimonie, D. Morphology and thermal properties of some green starch/poly(vinyl alcohol)/montmorillonite nanocomposites. *Cellul. Chem. Technol.* **2008**, *42*, 549−568.
(22) Ali, S. S.; Tang, X.; Alavi, S.; Faubion, J. Structure and physical properties of starch/poly vinyl alcohol/sodium montmorillonite nanocomposite films. *J. Agric. Food Chem.* **2011**, *59*, 12384−12395.
(23) Majdzadeh-Ardakani, K.; Nazari, B. Improving the mechanical properties of thermoplastic starch/poly (vinyl alcohol)/clay nanocomposites. *Compos. Sci. Technol.* **2010**, *70*, 1557−1563.
(24) Pascu, M. C.; Popescu, M. C.; Vasile, C. Surface modifications of some nanoocmposites containing starch. *J. Phys. D: Appl. Phys.* **2008**, *41*, 1−12.
(25) Southern Clay Products, Inc. Laponite: Performance additives. http://www.scprod.com/pdfs/Laponite%20brochure%20EN.pdf (accessed Dec. 4, 2011).
(26) Blanton, T. N.; Majumdar, D.; Melpolder, S. M. Microstructure of clay-polymer composites. Proceedings of the 47th Annual Denver X-ray Conference. August 3−7, 1998. Colorado Springs, CO, JCPDS − International Centre for Diffraction Data. Advances in X-ray Analysis, 1998; Vol. *42*, pp 562−568.
(27) Cummins, H. Liquid, glass, gel: The phases of colloidal Laponite. *J. Non-Cryst. Solids* **2007**, *353*, 3891−3905.
(28) Gaharwar, A. K.; Rivera, C. P.; Wu, C.-J.; Schmidt, G. Transparent, elastomeric and tough hydrogels from poly(ethylene glycol) and silicate nanoparticles. *Acta Biomater.* **2011**, *7*, 4139−4148.
(29) ASTM. Standard test methods for water vapor transmission of materials, E96-00. *Annual Book of ASTM Standards*; American Society for Testing and Materials: Philadelphia, PA, 2000.
(30) ASTM. Standard test method for tensile properties of thin plastic sheeting, D882-02. *Annual Book of ASTM Standards*; American Society for Testing and Materials: Philadelphia, PA, 2002.
(31) Batista, T.; Chiorcea-Paquim, A.-M.; Brett, A. M. O.; Schmitt, C. C.; Neumann, M. G. Laponite RD/polystyrenesulfonate nanocomposites obtained by photopolymerization. *Appl. Clay Sci.* **2011**, *53*, 27−32.
(32) Strawhecker, K. E.; Manias, E. Structure and properties of poly(vinyl alcohol)/Na+ montmorillonite nanocomposites. *Chem. Mater.* **2000**, *12*, 2943−2949.
(33) Yano, K.; Usuki, A.; Okada, A. Synthesis and properties of polyimide-clay hybrid films. *J. Polym. Sci., Part A: Polym. Chem.* **1997**, *35*, 2289−2294.
(34) Nair, S. H.; Pawar, K. C.; Jog, J. P.; Badiger, M. V. Swelling and mechanical behavior of modified poly(vinyl alcohol)/laponite nanocomposite membranes. *J. Appl. Polym. Sci.* **2007**, *103*, 2896−2903.
(35) Chivrac, F.; Pollet, E.; Dole, P.; Averous, L. Starch-based nanobiocomposites: plasticizer impact on the montmorillonite exfoliation process. *Carbohydr. Polym.* **2010**, *79*, 941−947.
(36) Lee, J. H.; Jung, D.; Hong, C. E.; Rhee, K. Y.; Advani, S. G. Properties of polyethylene-layered silicate nanocomposites prepared by melt intercalation with a PP-g-MA compatibilizer. *Compos. Sci. Technol.* **2005**, *65*, 1996−2002.
(37) Chivarac, F.; Gueguen, O.; Pollet, E.; Ahzi, S.; Makradi, A.; Averous, L. Micromechanical modeling and characterization of the effective properties in starch-based nano-biocomposites. *Acta Biomater.* **2008**, *4*, 1707−1714.
(38) Gaharwar, A. K.; Schexnailder, P. J.; Dundigalla, A.; White, J. D.; Matos-Pérez, C. R.; Cloud, J. L.; Seifert, S.; Wilker, J. J.; Schmidt, G. Highly extensible bio-nanocomposite fibers. *Macromol. Rapid Commun.* **2011**, *32*, 50−57.
(39) Shikinaka, K.; Aizawa, K.; Murakami, Y.; Osada, Y.; Tokita, M.; Watanabe, J.; Shigehara, K. Structural and mechanical properties of laponite-PEG hybrid films. *J. Colloid Interface Sci.* **2012**, *369*, 470−476.